

# Graphdiyne: A Metal-Free Material as Hole Transfer Layer To Fabricate Quantum Dot-Sensitized Photocathodes for Hydrogen Production

Jian Li,<sup>†,§</sup> Xin Gao,<sup>‡,§</sup> Bin Liu,<sup>†</sup> Qingliang Feng,<sup>‡</sup> Xu-Bing Li,<sup>†</sup> Mao-Yong Huang,<sup>†</sup> Zhongfan Liu,<sup>‡</sup> Jin Zhang,<sup>\*,‡</sup> Chen-Ho Tung,<sup>†</sup> and Li-Zhu Wu<sup>\*,†</sup>

<sup>†</sup>Key Laboratory of Photochemical Conversion and Optoelectronic Materials, Technical Institute of Physics and Chemistry, The Chinese Academy of Sciences, Beijing 100190, P.R. China

<sup>‡</sup>Center for Nanochemistry, Beijing Science and Engineering Center for Nanocarbons, Beijing National Laboratory for Molecular Sciences, College of Chemistry and Molecular Engineering, Peking University, Beijing 100871, P.R. China

## Supporting Information

**ABSTRACT:** Graphdiyne (GDY), a novel large  $\pi$ -conjugated carbon material, for the first time, is introduced as the hole transfer layer into a photoelectrochemical water splitting cell (PEC). Raman and ultraviolet photoelectron spectroscopic studies indicate the existence of relatively strong  $\pi$ - $\pi$  interactions between GDY and 4-mercaptopyridine surface-functionalized CdSe quantum dots, beneficial to the hole transportation and enhancement of the photocurrent performance. Upon exposure to a Xe lamp, the integrated photocathode produces a current density of nearly  $-70 \mu\text{A cm}^{-2}$  at a potential of 0 V vs NHE in neutral aqueous solution. Simultaneously, the photocathode evolves  $\text{H}_2$  with  $90 \pm 5\%$  faradic efficiency over three times and exhibits good stability within 12 h. All of the results indicate that GDY is a promising hole transfer material to fabricate a PEC device for water splitting by solar energy.

Water splitting by sunlight to produce hydrogen offers one of the most attractive solutions to deal with energy shortages and environmental remediation.<sup>1,2</sup> Photoelectrochemical (PEC) hydrogen production is a promising means because it can integrate the collection and conversion of solar energy into a photoelectrode.<sup>3-9</sup> A PEC cell is composed of two different electrodes, photocathode and photoanode, where electrons and holes can be collected and used to generate hydrogen and oxygen, respectively.<sup>4-6</sup> Given the advantages of excellent light-harvesting ability, high surface-to-volume ratios, quantum dots (QDs) have been considered as an alternative to molecular metal complexes and organic dyes for solar hydrogen evolution.<sup>10</sup> To date, sensitized photoelectrodes by QDs have mainly concentrated on photoanodes, where photogenerated electrons are injected into the conduction band of n-type semiconductor,<sup>3</sup> such as  $\text{TiO}_2$ . However, QD-sensitized photocathodes, running in a converse mode that photogenerated holes from QDs are transferred to the valence band of a p-type semiconductor,<sup>6</sup> are rarely reported. Spectroscopic studies have indicated that the light-stimulated electron of QDs can transfer to active sites smoothly, but hole transportation of QDs is relatively difficult,<sup>11</sup> suffering from the

much slower transfer rate than that of electrons. In this case, hole transfer is considered to be the crucial step for PEC water splitting. Therefore, developing suitable photocathode materials with advantage of high hole mobility, appropriate valence band position, ease of fabrication and high stability is the key to improve the PEC performance and stability.

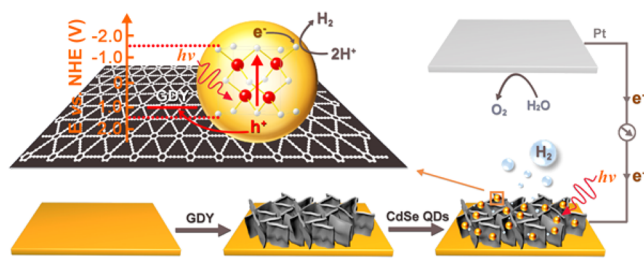
Graphdiyne (GDY), with highly  $\pi$ -conjugated structure, recently appears as a novel two-dimensional (2D) carbon nanomaterial, same as graphene.<sup>12</sup> According to the theoretical calculation,<sup>13</sup> the hole mobility of GDY is about  $10^4 \text{ cm}^2 \text{ V}^{-1} \text{ S}^{-1}$  order of magnitude, and the conductivity has been measured to be  $2.516 \times 10^{-4} \text{ S m}^{-1}$ , similar to that of single crystal Si. We envisioned that GDY could be employed as an excellent hole transfer material to construct a photocathode for hydrogen production. Unlike other p-type semiconductors used in the fabrication of photocathodes, such as  $\text{NiO}$ ,<sup>5</sup>  $\text{Cu}_2\text{O}$ ,<sup>7</sup> p-Si<sup>8</sup> and multielement  $\text{Cu}(\text{In,Ga})\text{Se}_2$ ,<sup>9</sup> the metal-free GDY has a rigid carbon network with delocalized  $\pi$ -system, natural band gap, remarkable electronic properties, and uniformly distributed pores. Owing to these attributes, GDY has shown interesting application in gas separation,<sup>14</sup> environmental cleaning,<sup>15</sup> Li storage,<sup>16</sup> and catalysis.<sup>17,18</sup> However, as far as we know, the attempt to use GDY as the hole transfer layer in PEC is yet unknown.

Here, we wish to fabricate the first photocathode employing GDY as hole transfer layer for hydrogen production in neutral water. Because the valence band potential of CdSe QDs ( $\sim 1.23 \text{ V vs NHE}$ )<sup>19</sup> is more positive than that of GDY ( $\sim 1.05 \text{ V vs NHE}$ ), the photogenerated holes from QDs can be injected into GDY thermodynamically. A schematic diagram of the integrated PEC cell and the corresponding interfacial migration process of photogenerated excitons are displayed in **Scheme 1**. Upon irradiation by 300 W Xe lamp, this assembled photocathode exhibits nearly  $-70 \mu\text{A cm}^{-2}$  photocurrent in 0.1 M  $\text{Na}_2\text{SO}_4$  (pH = 6.8) at an applied potential of 0 V vs NHE and simultaneously leads to a speed of  $27000 \mu\text{mol h}^{-1} \text{ g}^{-1} \text{ cm}^{-2}$  for hydrogen production at  $-0.20 \text{ V vs NHE}$ . The faradic efficiency up to 95% is obtained with an average of  $90 \pm$

Received: December 7, 2015

Published: March 10, 2016

**Scheme 1. Schematic Diagram of the PEC Cell, Consisting of the Assembled CdSe QDs/GDY Photocathode, Pt Wire as Counter Electrode, and Corresponding Interfacial Migration Process of the Photogenerated Excitons**



5%. The results demonstrate that GDY is a promising hole transfer material in PEC water splitting cell.

Typically, GDY was synthesized on a copper sheet via in situ growth method by a modified Glaser–Hay coupling reaction with hexaethynylbenzene (HEB) as precursor.<sup>20</sup> Detailed experimental procedures are available in the SI. SEM was employed to characterize the morphology of the as-prepared GDY film. As shown in Figure 1a, the GDY film showed an

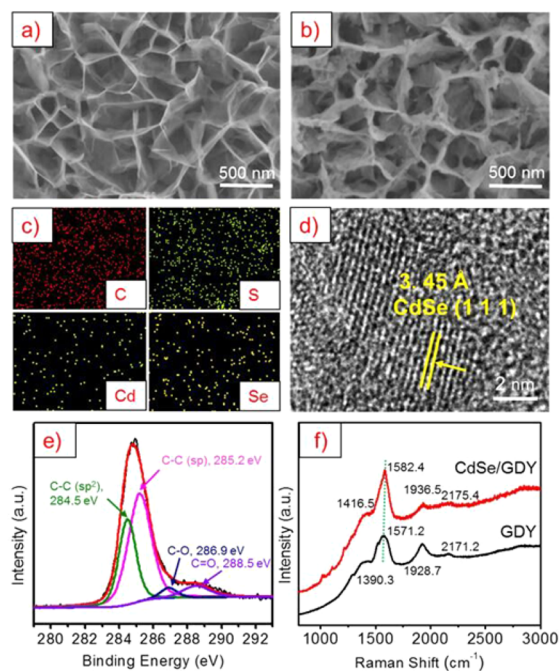


**Figure 1.** SEM images of (a) GDY film, (b) the assembled CdSe QDs/GDY film; (c) the elemental mapping of carbon, selenium, sulfur and cadmium by EDX spectra; (d) the HRTEM image of assembled CdSe QDs/GDY; (e) XPS spectra of GDY film; (f) Raman spectra of GDY and CdSe QDs/GDY films.

appearance of vertically regular cross-linked nanowalls, possessing large voids submicrometers in diameter, which was conducive to the adsorption of abundant CdSe QDs and sufficient contact with the electrolyte. Then, the CdSe QDs/GDY photocathode was fabricated in aqueous solution. In brief, nitric acid (2 M) was added into the solution of CdSe QDs to precipitate the QDs, separated with centrifugation and washed by deionized water for three times. Then, 4-mercaptopyridine surface-functionalized CdSe QDs solution was obtained by dispersing the precipitation in 4-mercaptopyridine aqueous solution (pH = 10.0). After immersing the GDY film into the 4-

mercaptopyridine surface-functionalized CdSe solution for 12 h, the CdSe QDs/GDY film was successfully prepared, presumably through the  $\pi$ - $\pi$  stacking between mercaptopyridine and GDY.<sup>21</sup> UV–vis diffuse reflectance spectra of the as-prepared CdSe QDs/GDY film displayed an enhanced absorbance starting at around 530 nm, consistent with that of untreated CdSe QDs solution (Figures S1 and S2). Furthermore, the SEM image presented the nanowalls appearance of the CdSe QDs/GDY electrode, but a much rougher surface than that of GDY (Figure 1b), and the corresponding elemental mapping further proved the uniform distribution of elements Cd and Se on the surface of GDY film (Figure 1c). Figure 1d displayed the HRTEM image of CdSe QDs/GDY. The defined lattice spacing of 0.345 nm is in line with the (111) crystalline planes of CdSe QDs. Surface morphology of GDY and CdSe QDs/GDY film electrodes were also investigated by atomic force microscopy. Consistent with SEM study, we could also observe the cross-linked nanowall appearance of GDY (Figure S3). Some visible particles in few to tens of nanometers range distributed over the CdSe QDs/GDY film were detected after absorbing CdSe QDs, an indicator of successful assembly of CdSe QDs.

The element composition and bonding structure of the photocathodes were further studied by XPS and Raman spectroscopy, respectively. In contrast to GDY films mainly containing elemental carbon, the CdSe QDs/GDY electrodes showed additional characteristic binding energy of Se, Cd, and S elements in the XPS spectra, which is in line with EDX analysis, shown in Figure S4. The peak at 284.8 eV for C 1s orbital could be observed for both GDY and CdSe QDs/GDY electrodes. After subtracting the Shirley background and fitting by Lorentzian and Gaussian functions, four subpeaks corresponding to  $sp^2$  (C=C) at 284.5 eV,  $sp$  (C≡C) at 285.2 eV, C=O at 288.5 eV, and C–O at 286.9 eV could be detected, respectively (Figure 1e).<sup>22</sup> The presence of O signal is due to the absorption of air in GDY. Beyond that, the Raman spectra of GDY film exhibits four notable peaks around 1387.8, 1568.5, 1923.2, and 2172.1  $cm^{-1}$ , respectively (Figure 1f), in line with previously reported data.<sup>12</sup> The peak at 1387.8  $cm^{-1}$  represents the breathing vibration of  $sp^2$  carbon domains in aromatic rings.<sup>23</sup> The peak at 1568.5  $cm^{-1}$  is attributed to the first-order scattering of the  $E_{2g}$  mode for in-phase stretching vibration  $sp^2$  carbon lattice in aromatic rings. The peaks at 2172.1 and 1923.2  $cm^{-1}$  are due to the vibration of conjugated diyne links (–C≡C–C≡C–). As for CdSe QDs/GDY film, the G band peak with a higher frequency region was observed, indicating some interactions occurred between GDY and mercaptopyridine surface-functionalized CdSe QDs. Similar phenomenon also took place in the  $sp$  C peak. With reference to the previous research in linear carbon chains,<sup>24</sup> the blue shift is due to the coupling with electron-withdrawing roles, thus implying the existence of  $\pi$ - $\pi$  stacking between GDY and mercaptopyridine surface-functionalized CdSe QDs.

The UPS, a surface analysis technique, that can be employed to confirm the highest occupied orbital of semiconductor thin film, was investigated. When GDY was covered by the mercaptopyridine surface-functionalized CdSe QDs, the HOMO level of CdSe QDs/GDY may be influenced by the interaction between GDY and CdSe QDs. Indeed, the HOMO position of CdSe QDs/GDY film was determined to be nearly –5.54 eV (Figure S6), higher than that of the pristine CdSe QDs ( $\sim$ –5.67 eV)<sup>19</sup> and lower than that of GDY ( $\sim$ –5.49 eV) (Figure S5). That is to say, the introduction of GDY layer

can reduce contact resistance between Cu and CdSe QDs active layer, which is conducive to hole collection and transfer. After CdSe QDs were presented on the surface of the GDY layer (Figure S7), a significant photoluminescence quenching and faster emission decay further suggested that GDY could extract photogenerated carriers from CdSe QDs efficiently. As the hole transfer layer, GDY, could improve the conductivity, decrease charge recombination, and reduce the resistance of the assembled photocathode.

Next, the open circuit potential (OCP) test was performed under dark and illuminated conditions to evaluate whether the GDY could serve as an effective hole transfer material in photocathode. As shown in Figure 2a, upon illumination, the

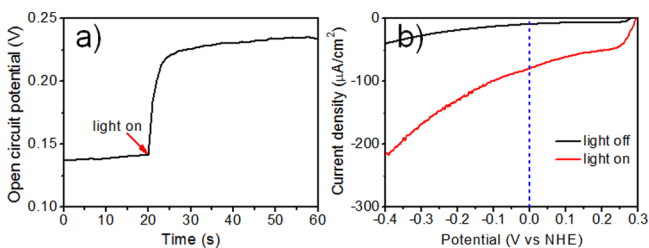


**Figure 2.** (a) Open circuit potential response of the CdSe QDs/GDY photocathode under dark and illuminated conditions (300 W Xe lamp). (b) LSV scanning from 0.3 to  $-0.4$  V at 2 mV/s with light off (black trace) and on (red trace) for CdSe QDs/GDY photocathode.

OCP shifted toward a more positive potential, which clearly demonstrated that holes generated from CdSe QDs can transfer to GDY in the assembled photocathode. LSV was conducted in 0.1 M  $\text{Na}_2\text{SO}_4$  aqueous solution scanning from 300 to  $-400$  mV with light on and off (Figure 2b), which revealed that CdSe QDs/GDY photocathode enabled generation of modest photocurrent under 300 W Xe lamp illumination with onset potential around 0.28 V vs NHE. Furthermore, photocurrent density of nearly  $-70 \mu\text{A cm}^{-2}$  could be obtained with an applied potential of 0 V vs NHE. The absence of either CdSe QDs or GDY in the integrated photocathode lowered the PEC activity markedly. Under identical conditions, the bare GDY electrode generated negligible photocurrent and spin-coated CdSe QDs on the copper substrate without the GDY hole transfer layer also resulted in a remarkable decline of photocurrent (Figure S8). These results indicated that the GDY buffer layer plays a crucial role in the hole transfer process, which may be attributed to its high hole mobility.<sup>25</sup>

Gas chromatography (GC) was used to confirm the amount of hydrogen evolved on CdSe QDs/GDY photocathode in 0.1 M  $\text{Na}_2\text{SO}_4$  at  $-0.20$  V vs NHE (Figure 3a). Irradiation of the

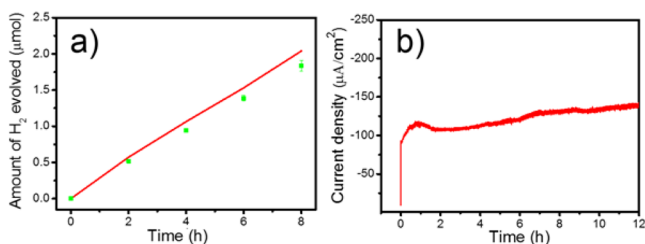


**Figure 3.** (a) Amount of evolved hydrogen and recorded charge carrier during photoelectrolysis. (b) Controlled potential electrolysis of the CdSe QDs/GDY photocathode during 12 h test.

photocathode by 300 W Xe lamp led to a speed of  $27000 \mu\text{mol h}^{-1} \text{g}^{-1} \text{cm}^{-2}$  for hydrogen production on the basis of CdSe QDs ( $1.45 \mu\text{g/cm}^2$ ). After 0.394 C charges passed through the external circuit, a faradic efficiency up to 95% was obtained with an average of  $90 \pm 5\%$  over three times. At the same time, the photogenerated holes from CdSe QDs were transferred to the counter electrode through the GDY layer for water oxidation,<sup>6</sup> which was confirmed by GC and Ocean Optics fluorescence-based oxygen sensor (Figure S9). According to the foregoing discussion, GDY, serving as an effective hole transfer material in the photocathode, is able to offer a high-performance PEC cell.

To our delight, the assembled photocathode maintained the constant photoelectrochemical activity in a 12 h test (Figure 3b). The Raman spectra of the photocathode after electrolysis displayed four prominent peaks at 1387.8, 1568.5, 1923.2, and  $2172.1 \text{ cm}^{-1}$ , respectively, suggesting that GDY was stable and undecomposed during photoelectrolysis (Figure S10). However, the peaks around 2172.1 and  $1923.2 \text{ cm}^{-1}$  after photoelectrolysis were more obvious and increased than that prior to photoelectrolysis, possibly a result of dissociation of some CdSe QDs from the GDY surface. The XPS spectra of the assembled photocathode after irradiation showed that the C 1s can still be deconvoluted in four types of circumstances containing sp ( $\text{C}\equiv\text{C}$ ) at 285.2 eV,  $\text{sp}^2$  ( $\text{C}=\text{C}$ ) at 284.5 eV,  $\text{C}=\text{O}$  at 288.5 eV, and  $\text{C}-\text{O}$  at 286.9 eV, respectively, while the proportions of  $\text{C}-\text{O}$  and  $\text{C}=\text{O}$  were slightly increased, which could be attributed to the absorption of more oxygen in GDY (Figure S11). Moreover, the characteristic binding energy of Se 3d and Cd 3d (Figures S12 and S13, respectively) from XPS analysis changed slightly due to dissociation of some CdSe QDs and then remained unchanged, indicating that the photocorrosion of CdSe QDs by the photogenerated holes was mostly avoided during irradiation. That is to say, the holes generated from CdSe QDs transferred to GDY rapidly, thus eliminating the excess holes in QDs efficiently. Therefore, the GDY plays a very important role in keeping the balance of photogenerated carriers from CdSe QDs for proton reduction and water oxidation in the PEC device (Scheme 1).

In addition, we prepared the CdS and CdTe QDs/GDY photocathodes in the same way, both of which yielded cathodic photocurrent and maintained the photoelectrochemical activity in the test for 4 h (Figure S14). Besides, we also grafted the CdSe and CdS QDs on the surface of GDY by repeating the successive ionic layer adsorption and reaction procedure, and all the photocathodes generated impressive photocurrent (Figure S15). These results hint that the GDY could be used as hole transfer layer with different loading methods for water splitting application.

In summary, the novel carbon material, GDY, as the hole transfer material, has been introduced to the PEC cell for the first time. The existence of relatively strong  $\pi-\pi$  interactions between GDY and mercaptopyrindine surface-functionalized CdSe QDs facilitates the hole transportation and photocurrent enhancement. Exposure of the assembled CdSe QDs/GDY photocathodes to Xe lamp leads to modest photoactivity and nearly  $90 \pm 5\%$  faradic efficiency for hydrogen production in a 12 h test. Our results are attributed to the higher hole mobility and stability of GDY. This study not only opens a new door to fabricate photocathodes using metal-free GDY as the hole transfer layer but also paves a new way to apply GDY in promising artificial photosynthesis for solar-to-fuel conversion.



## ■ ASSOCIATED CONTENT

## S Supporting Information

The Supporting Information is available free of charge on the ACS Publications website at DOI: 10.1021/jacs.5b12758.

Experimental details and data (PDF)

## ■ AUTHOR INFORMATION

## Corresponding Authors

\*lzwu@mail.ipc.ac.cn

\*jinzhang@pku.edu.cn

## Author Contributions

§These authors contributed equally.

## Notes

The authors declare no competing financial interest.

## ■ ACKNOWLEDGMENTS

This work was supported by the Ministry of Science and Technology of China (grant nos. 2014CB239402, 2013CB834505, and 2013CB834804), the National Natural Science Foundation of China (grant nos. 91427303, 21390404, 51432002, and 51373193), the Key Research Programme of the Chinese Academy of Science (KGZD-EW-T05), and the Chinese Academy of Science.

## ■ REFERENCES

- (1) (a) Gray, H. B. *Nat. Chem.* **2009**, *1*, 7. (b) Smith, A. M.; Nie, S. *Acc. Chem. Res.* **2010**, *43*, 190. (c) Chen, X.; Shen, S.; Guo, L.; Mao, S. *S. Chem. Rev.* **2010**, *110*, 6503. (d) Berardi, S.; Drouet, S.; Francas, L.; Gimbert-Surinach, C.; Guttentag, M.; Richmond, C.; Stoll, T.; Llobet, A. *Chem. Soc. Rev.* **2014**, *43*, 7501.
- (2) (a) Ran, J.; Zhang, J.; Yu, J.; Jaroniec, M.; Qiao, S. Z. *Chem. Soc. Rev.* **2014**, *43*, 7787. (b) Wu, L.-Z.; Chen, B.; Li, Z.-J.; Tung, C.-H. *Acc. Chem. Res.* **2014**, *47*, 2177. (c) Wang, H.; Zhang, L.; Chen, Z.; Hu, J.; Li, S.; Wang, Z.; Liu, J.; Wang, X. *Chem. Soc. Rev.* **2014**, *43*, 5234. (d) Osterloh, F. E. *Chem. Soc. Rev.* **2013**, *42*, 2294.
- (3) (a) Chen, H. M.; Chen, C. K.; Chang, Y. C.; Tsai, C. W.; Liu, R. S.; Hu, S. F.; Chang, W. S.; Chen, K. H. *Angew. Chem., Int. Ed.* **2010**, *49*, 5966. (b) Wang, G.; Yang, X.; Qian, F.; Zhang, J. Z.; Li, Y. *Nano Lett.* **2010**, *10*, 1088. (c) Robel, I.; Subramanian, V.; Kuno, M.; Kamat, P. V. *J. Am. Chem. Soc.* **2006**, *128*, 2385. (d) Kongkanand, A.; Tvrđy, K.; Takechi, K.; Kuno, M.; Kamat, P. V. *J. Am. Chem. Soc.* **2008**, *130*, 4007. (e) Kamat, P. V.; Tvrđy, K.; Baker, D. R.; Radich, J. G. *Chem. Rev.* **2010**, *110*, 6664.
- (4) Youngblood, W. J.; Lee, S.-H. A.; Kobayashi, Y.; Hernandez-Pagan, E. A.; Hoertz, P. G.; Moore, T. A.; Moore, A. L.; Gust, D.; Mallouk, T. E. *J. Am. Chem. Soc.* **2009**, *131*, 926.
- (5) (a) Ji, Z.; He, M.; Huang, Z.; Ozkan, U.; Wu, Y. *J. Am. Chem. Soc.* **2013**, *135*, 11696. (b) Li, F.; Fan, K.; Xu, B.; Gabrielson, E.; Daniel, Q.; Li, L.; Sun, L. *J. Am. Chem. Soc.* **2015**, *137*, 9153.
- (6) (a) Nann, T.; Ibrahim, S. K.; Woi, P. M.; Xu, S.; Ziegler, J.; Pickett, C. J. *Angew. Chem., Int. Ed.* **2010**, *49*, 1574. (b) Yang, H. B.; Miao, J.; Hung, S.-F.; Huo, F.; Chen, H. M.; Liu, B. *ACS Nano* **2014**, *8*, 10403. (c) Liu, B.; Li, X.-B.; Gao, Y.-J.; Li, Z.-J.; Meng, Q.-Y.; Tung, C.-H.; Wu, L.-Z. *Energy Environ. Sci.* **2015**, *8*, 1443. (d) Li, X.-B.; Liu, B.; Wen, M.; Gao, Y.-J.; Li, Z.-J.; Tung, C.-H.; Wu, L.-Z. *Adv. Sci.* **2015**, DOI: 10.1002/advs.201500282. (f) Ruberu, T. P. A.; Dong, Y.; Das, A.; Eisenberg, R. *ACS Catal.* **2015**, *5*, 2255.
- (7) (a) Paracchino, A.; Laporte, V.; Sivula, K.; Gratzel, M.; Thimsen, E. *Nat. Mater.* **2011**, *10*, 456. (b) Lin, C.-Y.; Lai, Y.-H.; Mersch, D.; Reisner, E. *Chem. Sci.* **2012**, *3*, 3482.
- (8) Seger, B.; Pedersen, T.; Laursen, A. B.; Vesborg, P. C.; Hansen, O.; Chorkendorff, I. *J. Am. Chem. Soc.* **2013**, *135*, 1057. (b) Ding, Q.; Meng, F.; English, C. R.; Cabán-Acevedo, M.; Shearer, M. J.; Liang, D.; Daniel, A. S.; Hamers, R. J.; Jin, S. *J. Am. Chem. Soc.* **2014**, *136*, 8504. (c) Ding, Q.; Zhai, J.; Cabán-Acevedo, M.; Shearer, M. J.; Li, L.

Chang, H.-C.; Tsai, M.-L.; Ma, D.; Zhang, X.; Hamers, R. J.; He, J.-H.; Jin, S. *Adv. Mater.* **2015**, *27*, 6511.

(9) Moriya, M.; Minegishi, T.; Kumagai, H.; Katayama, M.; Kubota, J.; Domen, K. *J. Am. Chem. Soc.* **2013**, *135*, 3733.

(10) (a) Wang, F.; Wang, W.-G.; Wang, X.-J.; Wang, H.-Y.; Tung, C.-H.; Wu, L.-Z. *Angew. Chem., Int. Ed.* **2011**, *50*, 3193. (b) Brown, K. A.; Wilker, M. B.; Boehm, M.; Dukovic, G.; King, P. W. *J. Am. Chem. Soc.* **2012**, *134*, 5627. (c) Han, Z.; Qiu, F.; Eisenberg, R.; Holland, P. L.; Krauss, T. D. *Science* **2012**, *338*, 1321. (d) Huang, J.; Mulfort, K. L.; Du, P.; Chen, L. X. *J. Am. Chem. Soc.* **2012**, *134*, 16472. (e) Li, Z.-J.; Fan, X.-B.; Li, X.-B.; Li, J.-X.; Ye, C.; Wang, J.-J.; Yu, S.; Li, C.-B.; Gao, Y.-J.; Meng, Q.-Y.; Tung, C.-H.; Wu, L.-Z. *J. Am. Chem. Soc.* **2014**, *136*, 8261. (f) Selinsky, R. S.; Ding, Q.; Faber, M. S.; Wright, J. C.; Jin, S. *Chem. Soc. Rev.* **2013**, *42*, 2963.

(11) (a) Tvrđy, K.; Frantsuzov, P. A.; Kamat, P. V. *Proc. Natl. Acad. Sci. U. S. A.* **2011**, *108*, 29. (b) Wilker, M. B.; Shinopoulos, K. E.; Brown, K. A.; Mulder, D. W.; King, P. W.; Dukovic, G. *J. Am. Chem. Soc.* **2014**, *136*, 4316. (c) Gimbert-Surinach, C.; Albero, J.; Stoll, T.; Fortage, J.; Collomb, M.-N.; Deronzier, A.; Palomares, E.; Llobet, A. *J. Am. Chem. Soc.* **2014**, *136*, 7655.

(12) Li, G.; Li, Y.; Liu, H.; Guo, Y.; Li, Y.; Zhu, D. *Chem. Commun.* **2010**, *46*, 3256.

(13) Long, M.; Tang, L.; Wang, D.; Li, Y.; Shuai, Z. *ACS Nano* **2011**, *5*, 2593.

(14) Jiao, Y.; Du, A.; Hankel, M.; Zhu, Z.; Rudolph, V.; Smith, S. C. *Chem. Commun.* **2011**, *47*, 11843.

(15) Gao, X.; Zhou, J.; Du, R.; Xie, Z.; Deng, S.; Liu, R.; Liu, Z.; Zhang, J. *Adv. Mater.* **2016**, *28*, 168.

(16) Huang, C.; Zhang, S.; Liu, H.; Li, Y.; Cui, G.; Li, Y. *Nano Energy* **2015**, *11*, 481.

(17) Wang, S.; Yi, L.; Halpert, J. E.; Lai, X.; Liu, Y.; Cao, H.; Yu, R.; Wang, D.; Li, Y. *Small* **2012**, *8*, 265.

(18) Thangavel, S.; Krishnamoorthy, K.; Krishnaswamy, V.; Raju, N.; Kim, S. J.; Venugopal, G. *J. Phys. Chem. C* **2015**, *119*, 22057.

(19) Huang, J.; Stockwell, D.; Huang, Z.; Mohler, D. L.; Lian, T. *J. Am. Chem. Soc.* **2008**, *130*, 5632.

(20) Zhou, J.; Gao, X.; Liu, R.; Xie, Z.; Yang, J.; Zhang, S.; Zhang, G.; Liu, H.; Li, Y.; Zhang, J.; Liu, Z. *J. Am. Chem. Soc.* **2015**, *137*, 7596.

(21) Geng, X.; Niu, L.; Xing, Z.; Song, R.; Liu, G.; Sun, M.; Cheng, G.; Zhong, H.; Liu, Z.; Zhang, Z.; Sun, L.; Xu, H.; Lu, L.; Liu, L. *Adv. Mater.* **2010**, *22*, 638.

(22) Estrade-Szwarckopf, H. *Carbon* **2004**, *42*, 1713.

(23) Tuinstra, F.; Koenig, J. L. *J. Chem. Phys.* **1970**, *53*, 1126.

(24) D'Urso, L.; Forte, G.; Russo, P.; Caccamo, C.; Compagnini, G.; Puglisi, O. *Carbon* **2011**, *49*, 3149.

(25) Xiao, J.; Shi, J.; Liu, H.; Xu, Y.; Lv, S.; Luo, Y.; Li, D.; Meng, Q.; Li, Y. *Adv. Energy Mater.* **2015**, *5*, 1401943.